Prepared for
Ballistic Systems Division
Air Force Systems Command
under Contract AF 04(694)-222
(Project TRAP)

R63SD1042

PERFORMANCE EVALUATION OF TRAP IMAGE ORTHICON SYSTEM

R. L. Gulatsi

SPACE SCIENCES LABORATORY
GENERAL ELECTRIC
MISSILE AND SPACE DIVISION

SPACE SCIENCES LABORATORY

AEROPHYSICS SECTION

PERFORMANCE EVALUATION OF TRAP IMAGE ORTHICON SYSTEM

by

R. L. Gulatsi

The work described in this report was supported by the Ballistic Systems Division, Air Force Systems Command, United States Air Force, under Contract AF 04(694)-222 (Project TRAP)

R63SD1042
December 21, 1963

MISSILE AND SPACE DIVISION

GENERAL ELECTRIC

TABLE OF CONTENTS

LIST OF FIGURES

I. INTRODUCTION

This report describes performance data obtained by the General Electric Missile and Space Division on an image orthicon system used for radiation measurements against re-entry vehicles. Effort described herein was performed as a portion of Project TRAP for the Ballistic Systems Division, Air Force System Command, Norton AFB, California, under Contract AF04(694)-222.

Specifically presented is a description of the image orthicon system, along with data derived from experiments performed to investigate system performance achievable in the point target radiometric application.

II. HISTORY

The image orthicon tube offers a potential sensitivity advantage of at least 10 db over a film instrument of equivalent frame rate and optics. For a re-entry measurements program such as TRAP, this sensitivity is extremely attractive, particularly to optimize probability of data acquisition against low observable vehicles at high target altitude. From a systems standpoint, utilization of an imaging instrument is also desirable since it provides high angular resolution without the need for extremely precise instrument pointing.

Recognition of image orthicon potentiality led, in late 1961, to the installation of an S-10 image orthicon radiometric system as a portion of the General Electric equipment aboard the TRAP KC135 aircraft. Limited operational experience was then available on the specific operational capabilities of the image orthicon when used as a radiometer against point targets. Experimental work completed by General Electric at that time, however, predicted that image orthicon point target radiometry would entail different considerations than use against "studio" extended scenes.* For example, resolution for point images was noted as involving different considerations than those specifications normally given for the image orthicon.

*Photoelectric Observatory Report No. 1, John F. Spalding, General Engineering Laboratory, General Electric Company, Schenectady, N. Y., October 1960.

As described in the referenced document, normally-quoted resolution figures are usually a measure of the information capacity of a noisy channel, whereas point target image size is proportional to the intensity of the incident radiation. This is the now well-known "blooming" effect noted when observing point objects.

Early operation of the image orthicon aboard the KC135 aircraft quickly verified that operation against re-entry vehicle targets involves different considerations than those pertinent to the normal "studio" extended scene application. This spelled out a need for experimentation with the system to define its point target performance. In particular, definition and optimization of achievable combinations of sensitivity, dynamic range, and resolution in terms of available system adjustments was called for.

Early in 1963, program requirements placed increased emphasis on achieving maximum performance from the image orthicon system. This led to the decision to temporarily remove this equipment from the KC135 aircraft to a location where system-optimization experiments could be performed. The General Electric WSMR TRAP V ground station, located at Holloman Air Force Base, was chosen for this purpose. This site was picked, rather than the laboratory, since it also allows use of the instrument for active data gathering during the experimental interval.

Experiments have been completed which give a reasonable understanding of presently achievable point target capabilities and corresponding adjustment criteria. A description of the experimental results, along with a description of the system, is contained in the following sections of this report.

III. SYSTEM DESCRIPTION

Figure 1 diagrams the system. The 10-inch lens provides a nominal 5-degree by 7-degree field of view.

The optics, as shown, include an automatic iris, which consists of a liquid contained between movable clear plates. This component provides

attenuation up to a factor of 1000, which is controlled by moving the plates to control the path length through the liquid. The motion is servo-controlled by the video output so that the maximum video amplitude is held at one volt.

The automatic iris was provided at initial equipment installation to extend frame-to-frame dynamic range. Operational experience, however, indicated that its use was undesirable, since undesired strong targets reduced system sensitivity below the detection threshold for desired weak targets. This fact, coupled with an insertion loss reducing system sensitivity by a factor of almost two, resulted in removal of the component.

Camera, sweep, and video circuits are straightforward. Data recording is accomplished by photographing a display panel containing cathode ray tubes for video display and ancillary indicators for display of other data such as timing. The recording camera is synchronized to the television raster, and records one out of three television frames. This provides a 10 frame-per-second recording data rate for the 30 frame-per-second interlaced TV raster employed.

The video information is displayed on a horizontal A-scope which presents vido amplitude versus horizontal sweep, a vertical A-scope which presents video amplitude versus vertical sweep, and a C-scope. The latter is a standard television monitor display. Radiometric data is obtained from the A-scopes, which are calibrated in terms of video pulse amplitude versus front optic irradiance. Use of the two A-scopes decreases the probability of superimposed video pulses from a multi-target complex. The C-scope is used for geometric swarm dispersion data and general event identification. It also provides a "built-in" boresite camera for the A-scopes. Figure 2 pictures a typical display presentation, obtained from the TRAP KC135 aircraft against a multi-object re-entry target.

An electronic cross-hatch generator provides an aid to angular position interpretation on the C-scope. A shading correction generator is also provided. This gives vertical and horizontal saw tooth and parabolic waveforms which may be added to the video so as to decrease the effects of sensitivity variation over the image orthicon retina.

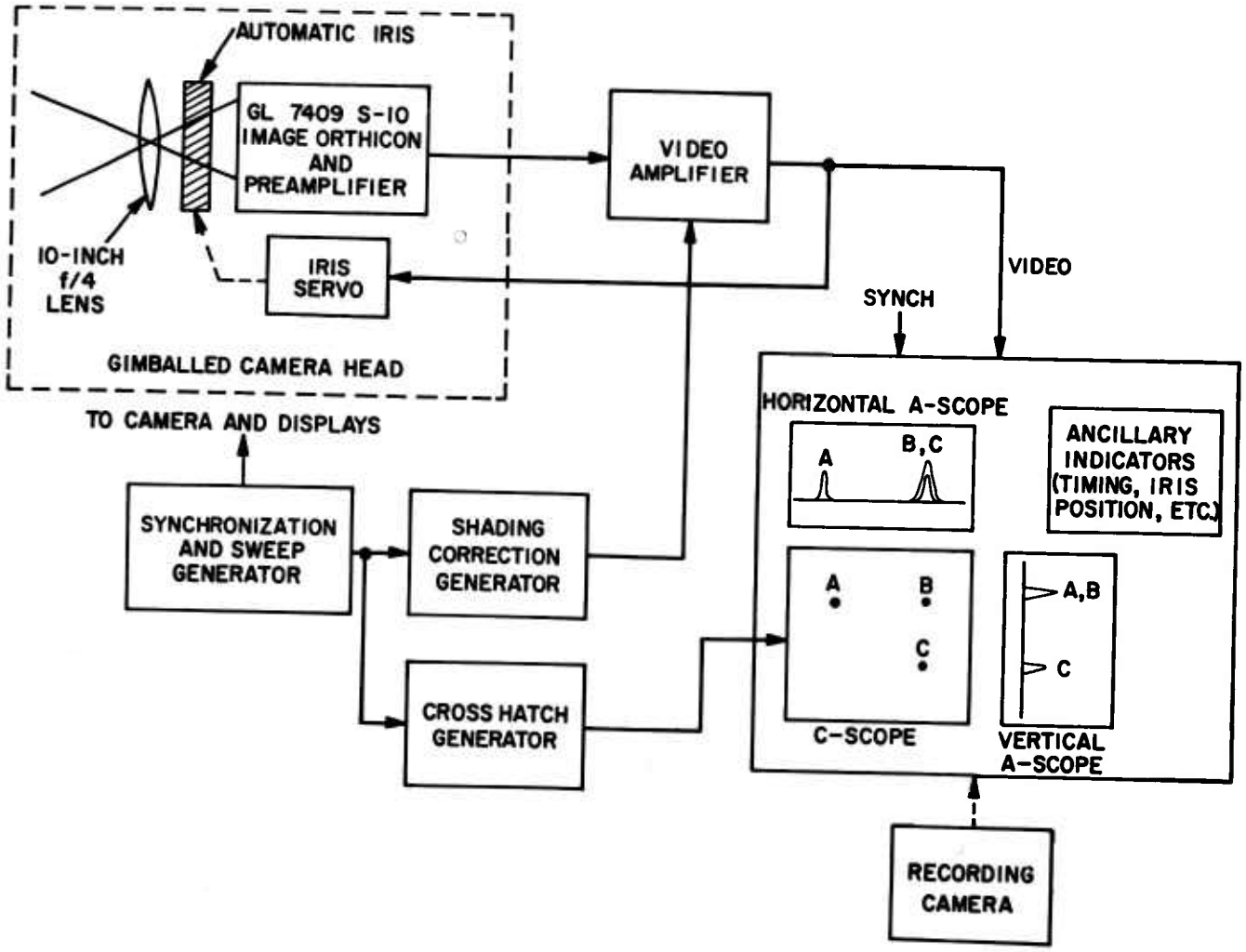

Figure 1. Image Orthicon System

The system, as installed at the WSMR General Electric TRAP V field site, is shown in Figure 3. Shown, from left to right, are the electronic circuitry racks, the data display and recording panel, and the camera assembly.

For the experimental program, additional circuitry was added to pulse the photocathode for reciprocity tests. This equipment, and its interconnection with the original image focus circuit, is diagrammed in Figure 4, and pictured in Figures 5 and 6.

System calibration is accomplished by use of a point source aperture and a standard tungsten bulb. The bulb is operated at a true temperature of 2800 degrees Kelvin. Source intensity is varied by placing appropriate neutral-density filters in front of the point aperture. Radiant intensity in the S-10 bandpass is taken as the product integral of the tungsten spectral radiation and the S-10 spectral bandpass, i.e., $\int S_{10\,(\lambda)}\, J_{W\,(\lambda)}\, d\lambda$. The range squared factor is then applied to convert to the front optic irradiance product integral, $\int S_{10(\lambda)}\, H(\lambda)\, d\lambda$. Calibration consists of determination of A-scope pulse amplitude and pulse width versus the front-optic irradiance product integral.

For the aircraft installation, calibration is accomplished by locating the calibration source and an appropriate power cart at a convenient point with respect to the aircraft on the flight line. At the WSMR TRAP V site, the calibration source is located in a building at a distance of 400 feet from the equipment under calibration.

Calibration is performed against a sky background which corresponds to that expected during the actual data acquisition interval. A dark night sky is the usual case.

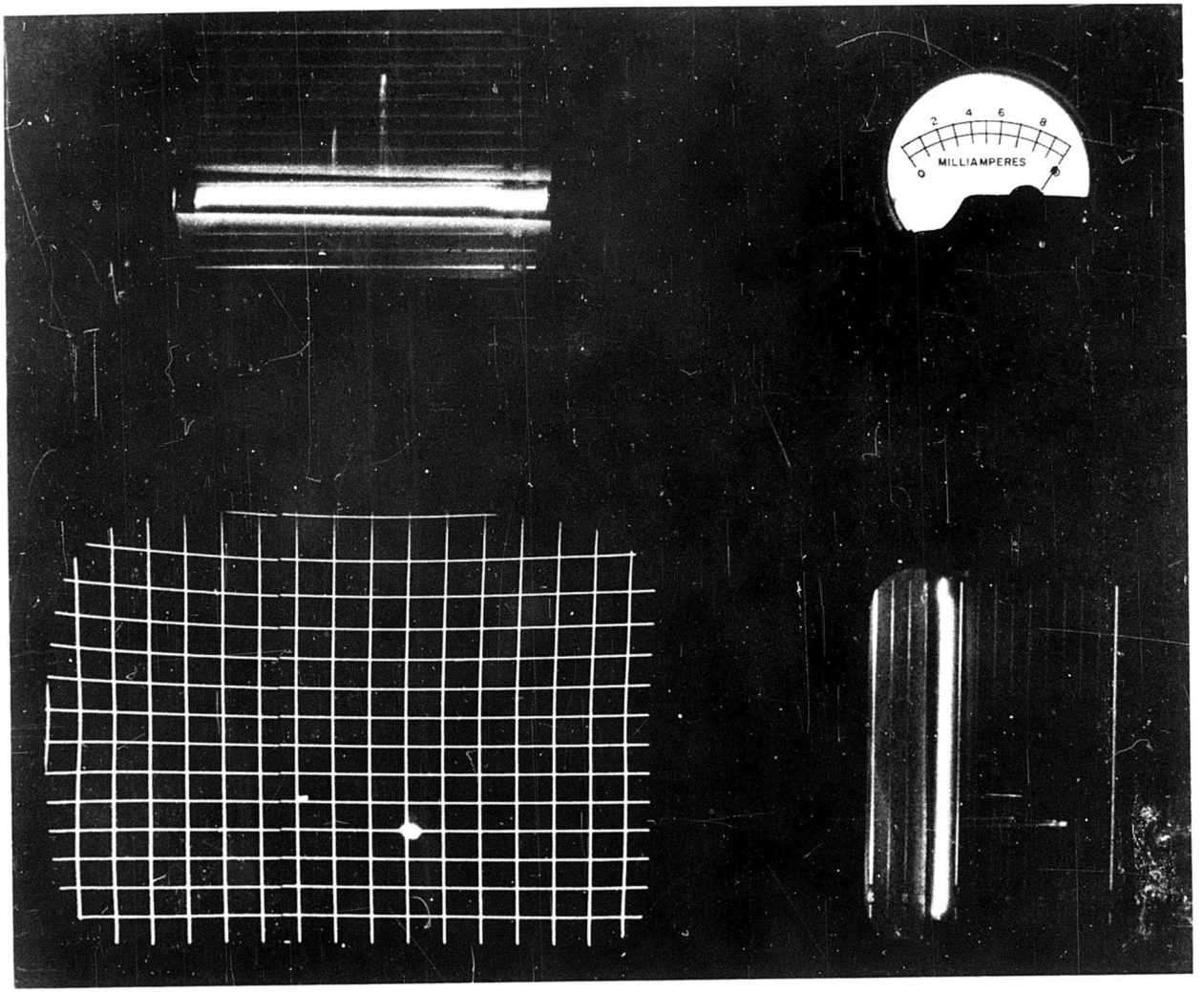

Figure 2. Typical Image Orthicon Display Presentation

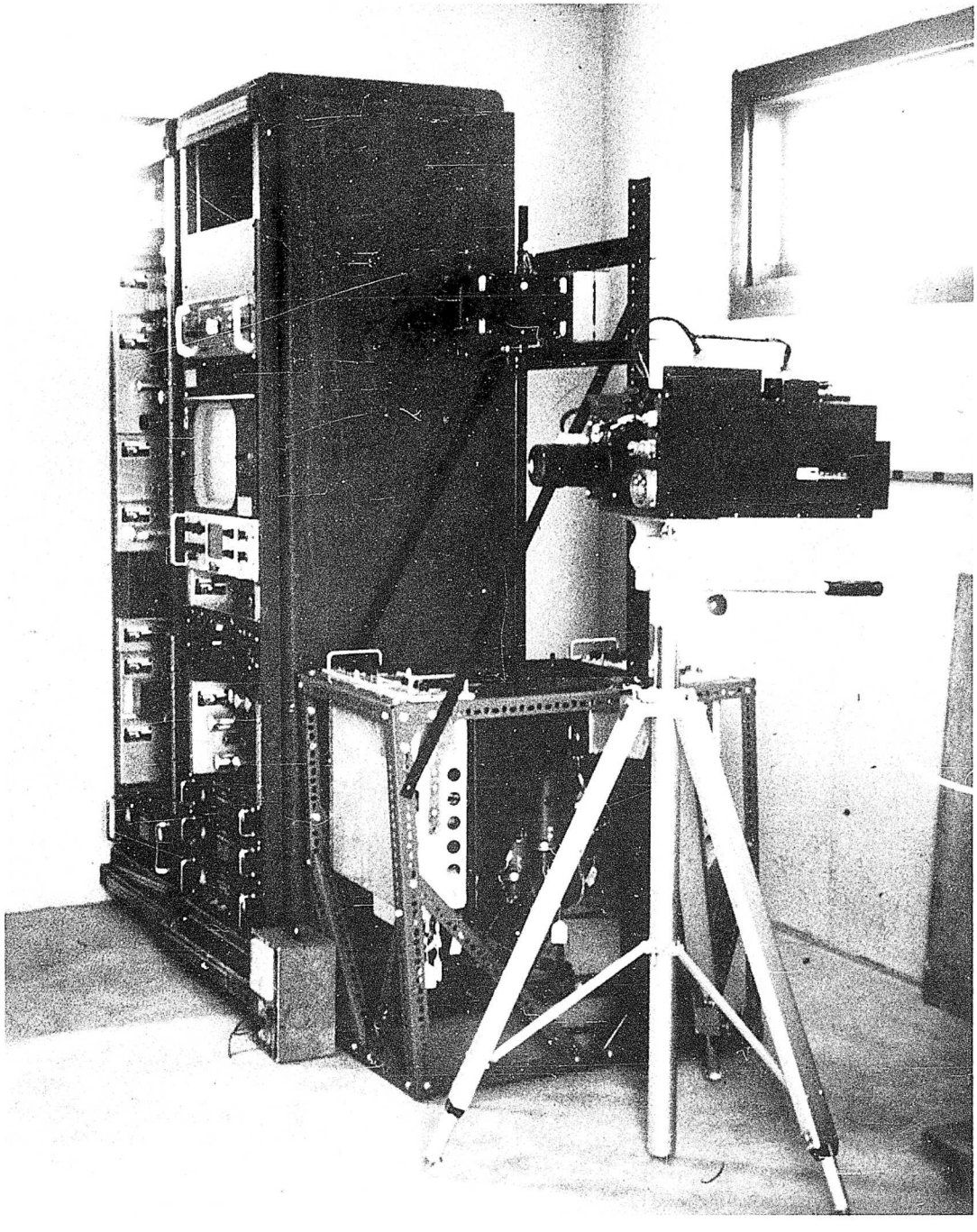

Figure 3. Image Orthicon System Installation at WSMR TRAP V Field Site

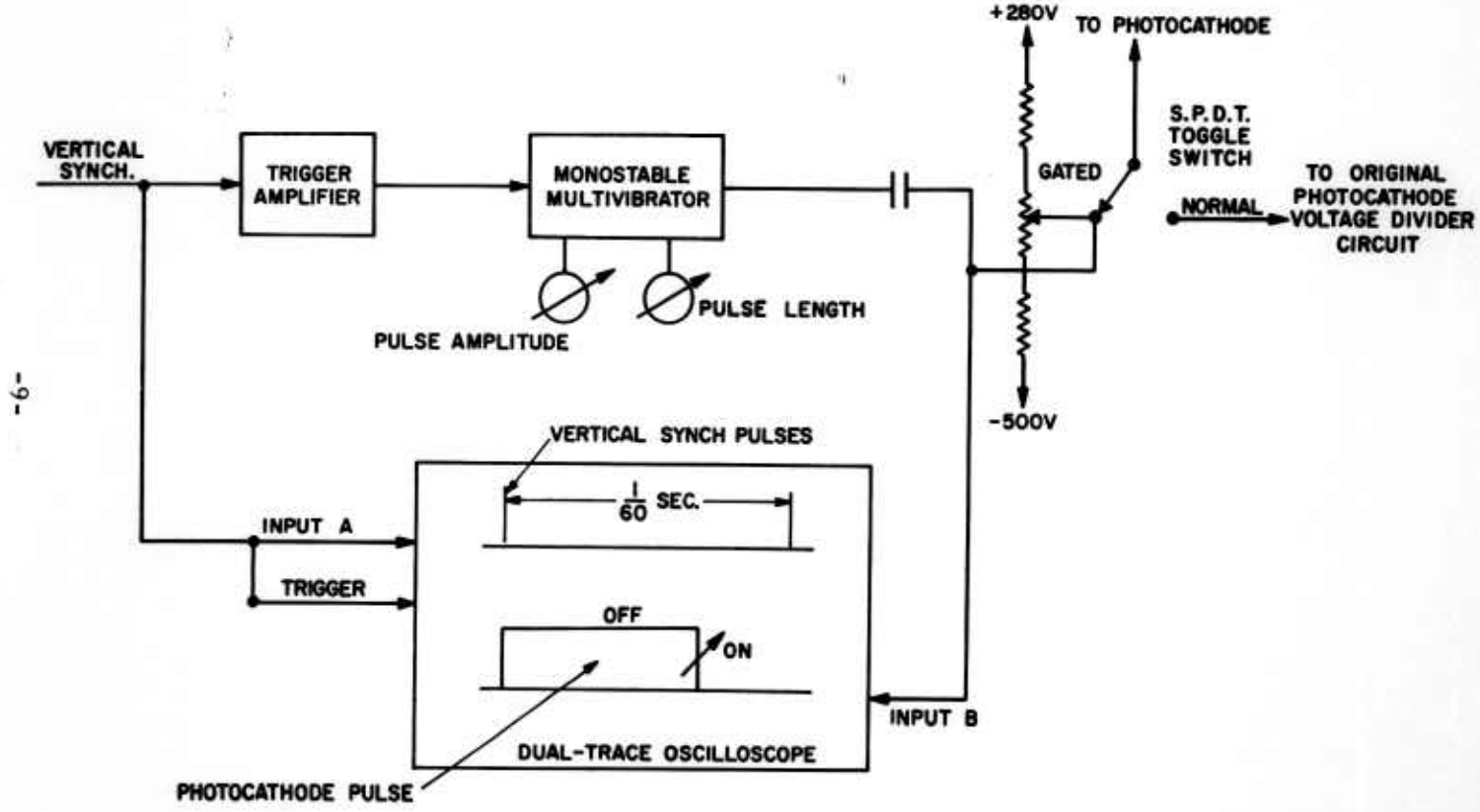

Figure 4. Photocathode Gating Circuitry

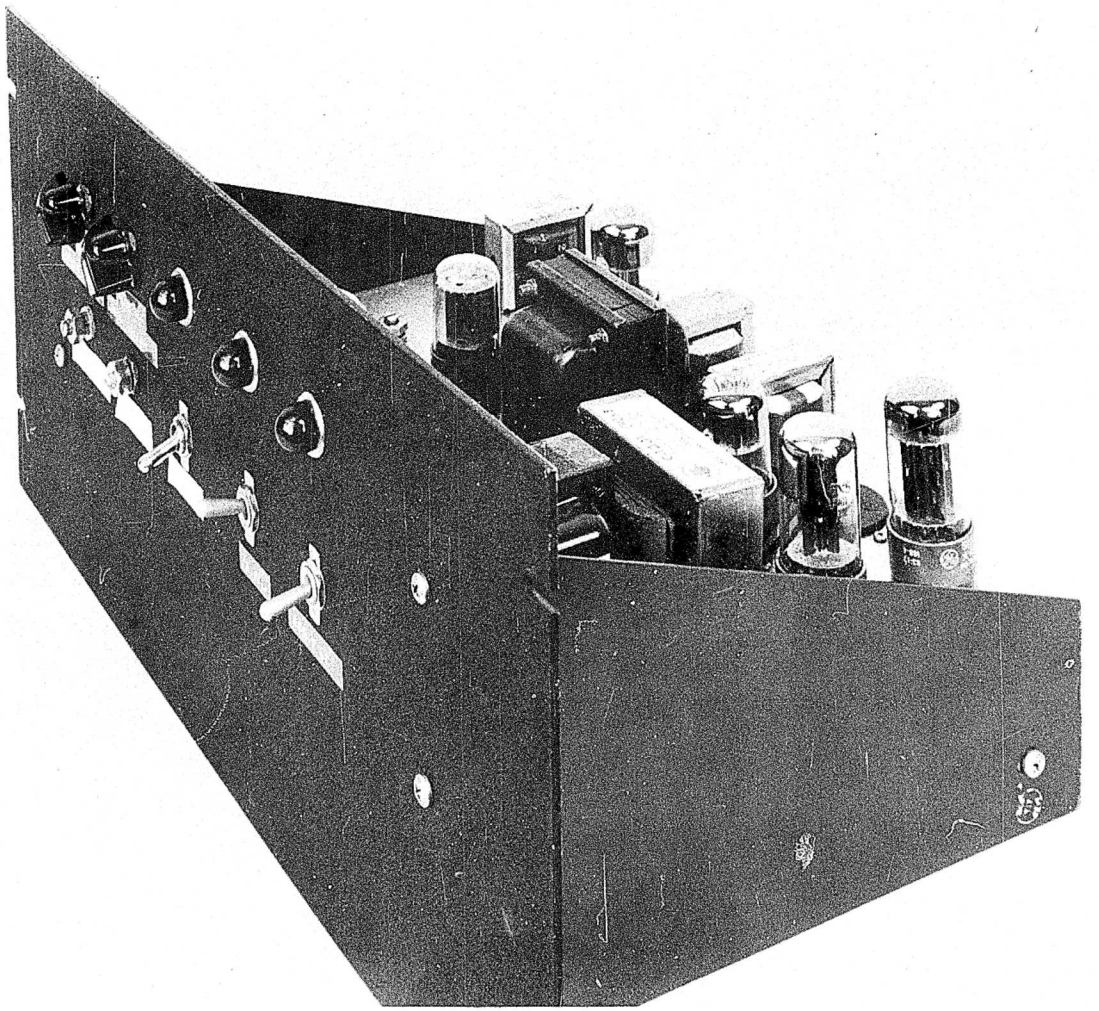

Figure 5. Trigger Amplifier and Pulse Generator - Front View

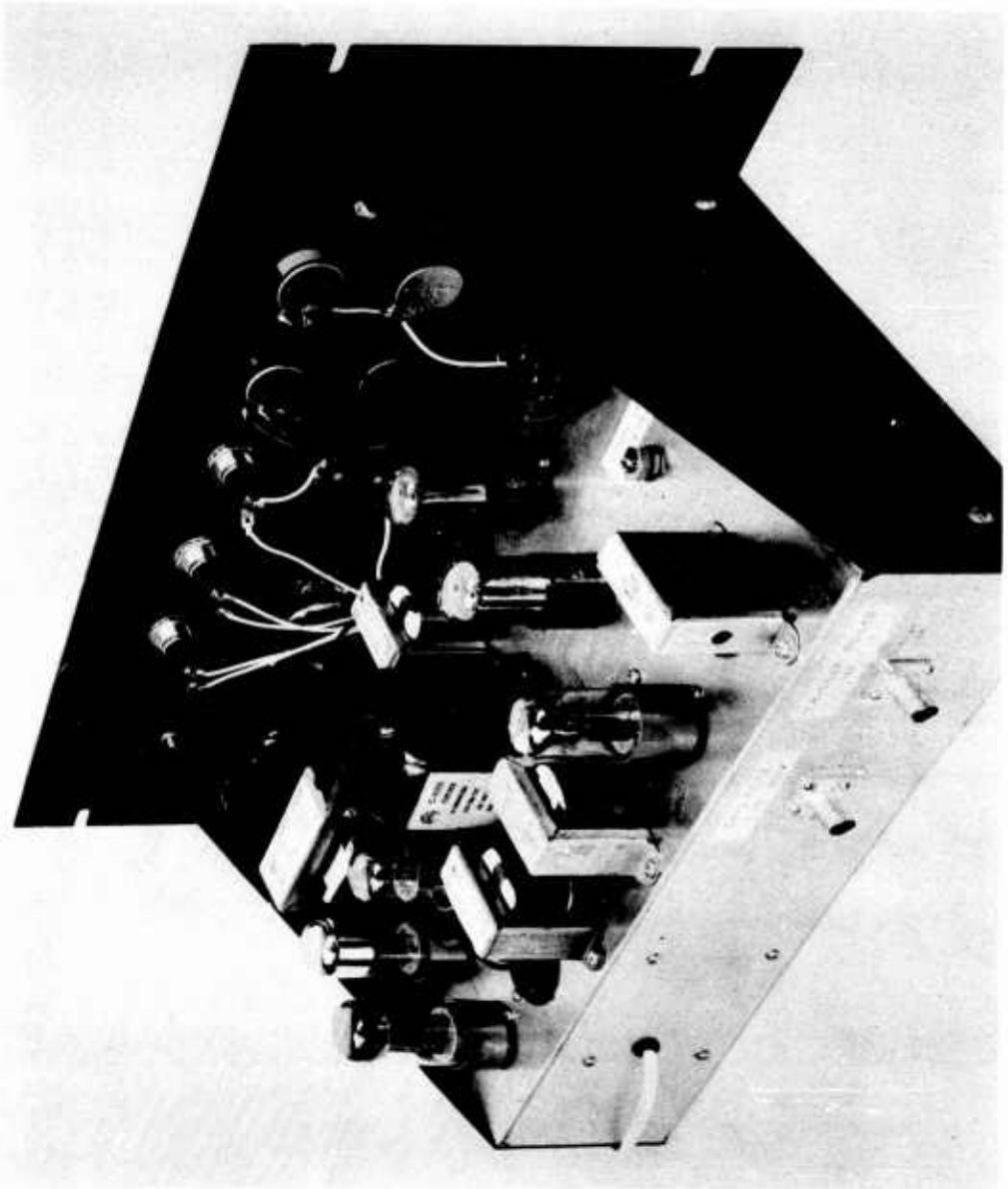

Figure 6. Trigger Amplifier and Pulse Generator, Rear View

IV. EXPERIMENTAL PROGRAM

A. Goals and Scope

Goals for the image orthicon experiments, as defined at their onset, are listed below.

1. Review the theoretical aspects of image orthicon operation.
2. Determine achievable point and line target dynamic range/resolution/sensitivity combinations as a function of target voltage and beam current.
3. Determine radiometric calibration accuracies
   a. Stability
   b. Sensitivity variation across retina
4. Establish suitable field-of-view calibration techniques and accuracy thereof.
5. Investigate reciprocity effects for integration times of less than one frame.
6. Specify proper field adjustment, calibration and operational procedures. Document in an up-dated Instruction Manual.
7. Document results of experiments in a Final Report.

Program scope was established as that of defining performance of the present system rather than modification thereof to upgrade achievable performance. For meeting Goal 5, however, additional circuitry was constructed to allow photocathode pulsing. This was felt warranted since considerable resolution degradation was noted in KC135 operation due to image smearing under imperfect tracking, and a direct measure of system performance at shorter exposure times was deemed cogent.

B. Summary of Test Results

Present system capability and according adjustment criteria, for the point target case, have been reasonably well defined by the experiments performed.

The effect of beam current and target voltage adjustment on dynamic range, resolution, and sensitivity were established by calibrating the system

at three levels of beam current at each of the target voltages +2, +5, +8, and +10 volts.* Based upon these experiments, operating conditions of +2 volts target voltage and "medium" beam current (beam current test point voltage = -77 volts) have been chosen.

Sensitivity variation across the image orthicon retina was measured, both with and without use of shading correction video waveforms. No appreciable reduction of sensitivity variation was noted through use of the shading correction generator. This may be due to the limited time allotted to experimentation with this component in accord with the required overall scheduling of the program. Sensitivity over most of the retina surface is within 85% of the value achieved at the center. A dropoff to about 75% is noted at the extreme edges.

Reciprocity tests indicated that approximate reciprocity is achieved for integration times of less than about 60% of a frame. Reciprocity falls off at greater integration times, apparently since image focus also falls off under these conditions. This appears due to the need for a simple change in the photocathode pulsing circuitry rather than to image orthicon tube performance per se. The revised photocathode bias circuitry used in pulsing, however, provides a superior image focus under all conditions as compared with the circuitry provided with the original equipment. This condition appears responsible for the degraded system sensitivity noted in previous operation aboard the TRAP aircraft.

System performance measured at the operating conditions of +2 volts target voltage and "medium" beam current is summarized in Table I.

"Useful dynamic range" figures noted in Table I must be interpreted with caution. They are defined as the range of input irradiances between twice the NEFD and the knee of the A-scope deflection vs. input irradiance curve. Exact definition of the knee of the curve is subject to interpretation and estimate; also operation somewhat above the knee may allow sufficient curve slope to perform radiometric measurements.

*Target voltages of less than + 2 volts could not be obtained from the original voltage control circuit. Later tests at +1.0 volt target potential are planned after appropriate circuit modification.

Tests performed pertinent to the radiometric stability-definition portion of Goal 3 indicate that improvement is needed in this area. It was observed that control settings, particularly those associated with beam landing and alignment, are critical in adjustment, subject to short-term drift, and must be "touched up" frequently during operation to maintain a constant overall system transfer function. It was noted that up to a 1.5 to 1 change in A-scope pulse amplitude, for a fixed input irradiance, may be occurred over a five to ten minute period if the landing and beam alignment controls are not readjusted over this time interval. This drift provides estimated radiometric uncertainty of perhaps ± 35% to ± 50% dependent on the calibration transfer function in question. Further check-out and testing is required to define the cause of the instability and to allow according corrective action to be taken .

Experiment plans and calibration equipment requirements were defined for the field-of-view calibration tests of Goal 4, and also for performance of experiments against line targets. Available time, however, did not allow implementation of these experiments.

Revised image orthicon calibration and operating instructions have been issued, taking into account the data derived from the experiments performed.

V. CONCLUSIONS AND RECOMMENDATIONS

Experiments have been completed which define the point target radiometric capability of the image orthicon equipment as it is now mechanized. The condition of degraded sensitivity, as noted in previous on-aircraft operation, has been corrected.

Presently-achievable performance provides a best sensitivity of about 2×10^{-14} watts/cm^2-S10. Maximum point target resolution is 250 elements, occurring at or near the minimum input signal level. Blooming decreases resolution to between about 180 and 100 elements, dependent on system adjustment, at the upper end of the dynamic range. Dynamic ranges of between about 20 and 60 were measured, dependent on the system operational mode in use.

TABLE I. SUMMARY OF PRESENT SYSTEM PERFORMANCE

	Sensitivity (NEFD) watts/cm^2-S10	Useful Dynamic Range*	Resolution elements at 2 x NEFD	Resolution at H_{max}
1. Photocathode gated, 40% on-time	3×10^{-14}	18.3	250	182
2. Photocathode gated, 60% on-time	1.8×10^{-14}	44.5	250	150
3. Photocathode gated, 80% on-time	1.8×10^{-14}	58.5	250	93
4. No photocathode gating, 100% on-time (Original image focus circuitry)	9×10^{-14}	36.6	250	65

*Useful Dynamic Range = $\frac{H_{min}}{H_{max}} = \frac{2 \times \text{NEFD}}{\text{Knee of } H_{in} \text{ vs. } \epsilon_o \text{ curve}}$

Capability for operation at integration times of less than one frame was established, along with the indication that reciprocity should hold reasonably well under this condition.

It was noted that the system exhibits an overall gain drift. This causes, for a fixed input irradiance, a change by a factor of up to about 1.5 in output video pulse amplitude over a five to ten minute period. A radiometric uncertainty of up to perhaps 40% to 50% is predicted due to this effect. It has not been definitely established at this time whether this drift is inherent, or simply due to a defective component or subsystem.

Continuing experimental effort at the TRAP V site, in the following order of priority and chronological implementation, is planned.

1. Perform checkout and testing as required to isolate reasons for system gain drift and to reduce this effect to a minimum. Measure short and long term radiometric calibration accuracy under this condition.

2. Perform experiments pertinent to field of view calibration and drift.

3. Perform experiments pertinent to evaluation of system operation against line targets.

Relocation of the image orthicon to the KC135 aircraft at this time is not recommended, primarily due to the existing radiometric instability.

Use of an S-20 tube for the remaining experiments, along with an S-20 recheck of the previously obtained S-10 data, is being implemented. Exploratory S-20 tests have indicated a factor of up to 50 in detectability increase against a 2800^{o}K target, as compared to the S-10 tube.

Point and line target experimentation with dynamic range extension techniques recently developed by the General Electric Company is also contemplated. These, through servoing of beam current in accord with video pulse amplitude, have demonstrated a factor of improvement of 100 or more in achievable dynamic range against extended scenes. The dynamic range thus gained is point-to-point within a given frame, which is extremely attractive to the system requirement which is present.

APPENDIX I. DETAILED TEST RESULTS

1. Dynamic Range/Sensitivity/Resolution as a Function of Beam Current and Target Voltage

The relative effects of target voltage and beam current on achievable combinations of S-10 point target dynamic range/resolution/sensitivity were measured, using the GL 7409 image orthicon tube. This was done by determining the system video output and resolution, as a function of front optic irradiance, at three levels of beam current at each of the target voltages +2, +5, +8, and +10 volts. Beam currents were chosen as "low" (just discharges highlights), "high" (maximum usable), and "medium" (midway between low and high). These are obtained at image orthicon gun control grid test point voltages of -90, -77, and -58 volts, respectively.

System setup was made per adjustment which prevents data distortion due to limiting in the A-scopes and video amplifier.

Tests were made at 100% integration time, using the originally supplied image focus circuitry.

System response and resolution were measured against a point source located 70 feet from the image orthicon lens. The source consisted of a tungsten bulb operated at 2800 degrees Kelvin true temperature and located behind an aperture of 0.1 x .0615 inches. Source radiant intensity was varied by placing appropriate neutral density filters in front of the aperture plate. Front optic irradiances thus obtained was computed as the product integral of the tungsten spectral irradiance and the S-10 spectral response.

Tests were made against a clear night sky, typical of that to be expected during re-entry test observations. System noise, as measured under capped lens conditions, was not significantly increased by background radiation.

Data taken consists of horizontal A-scope pulse amplitude and resolution vs. front optic irradiance, and is shown in Figures 7, 8, 9, and 10.

Resolution was defined by dividing the total A-scope deflection width by the video pulse width at half-power amplitude. Measurement of pulse

width was accomplished with a millimeter scale, using a factor of 5 expansion in A-scope horizontal deflection to increase ease and accuracy of measurement. Resolution measurements thus obtained are considered reasonably valid at the wider pulse widths corresponding to strong signals, but become relatively difficult to interpret at the narrow pulse widths corresponding to small input signals. A general topping out of resolution at some 250 elements under all adjustment conditions was observed, the data shown thus is extrapolated to this value at the smaller signal levels.

NEFD's shown on the curves are indicative of relative sensitivity rather than as absolute values. The automatic iris had not yet been removed when this data was taken, and the iris insertion loss appears in the results. Also, these NEFD's were obtained by straight line extrapolation to the noise baseline from the minimum measured calibration point. Later and more detailed absolute system transfer function measurements indicated that a non-linear extrapolation was pertinent; this results in lower NEFD's. Absolute system sensitivity is discussed later in this report.

Overall dynamic range is defined, for the comparative purposes applicable here, as the irradiance value at the knee of the A-scope pulse amplitude vs. irradiance curve divided by the NEFD. This, as an absolute value, must be treated with caution. In particular, exact definition of the knee of the various curves is subject to interpretation and estimate, and sufficient slope may exist beyond the knee for radiometric use.

Examination of the data obtained leads to the following observations.

1. Point target dynamic range is primarily dependent upon beam current. Achievable dynamic ranges, per the aforementioned definition, vary from a minimum of about 15 for low beam current to a maximum of 60 or more for high beam current.

2. Dynamic range is degraded by raising target voltage, particularly to values above 8 volts.

3. For target voltages between 2 and 5 volts, as applicable to best dynamic range, system sensitivity is primarily dependent on beam current.

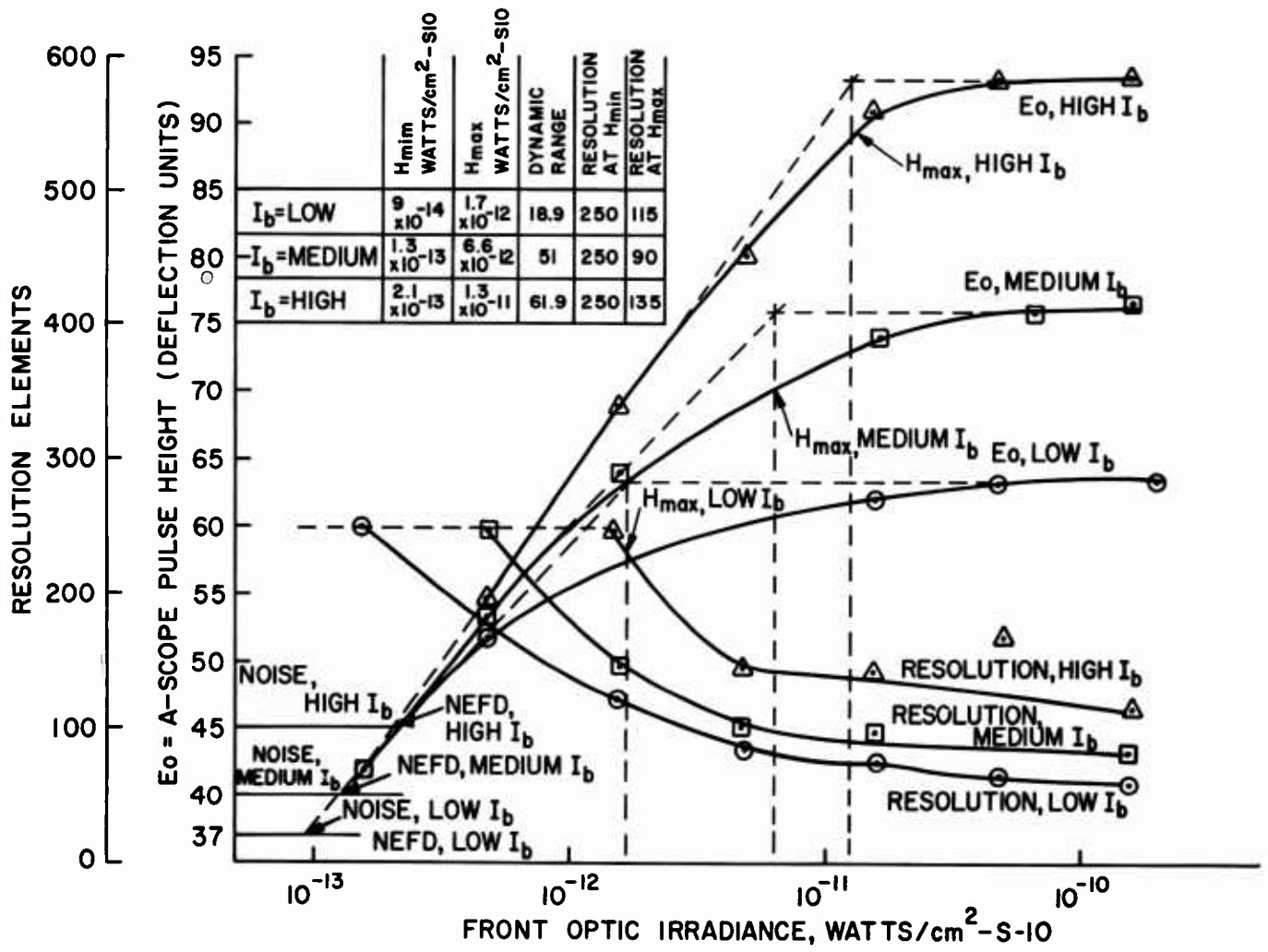

Figure 7. System Transfer Functions, ϵ_T = + 2.0 Volts

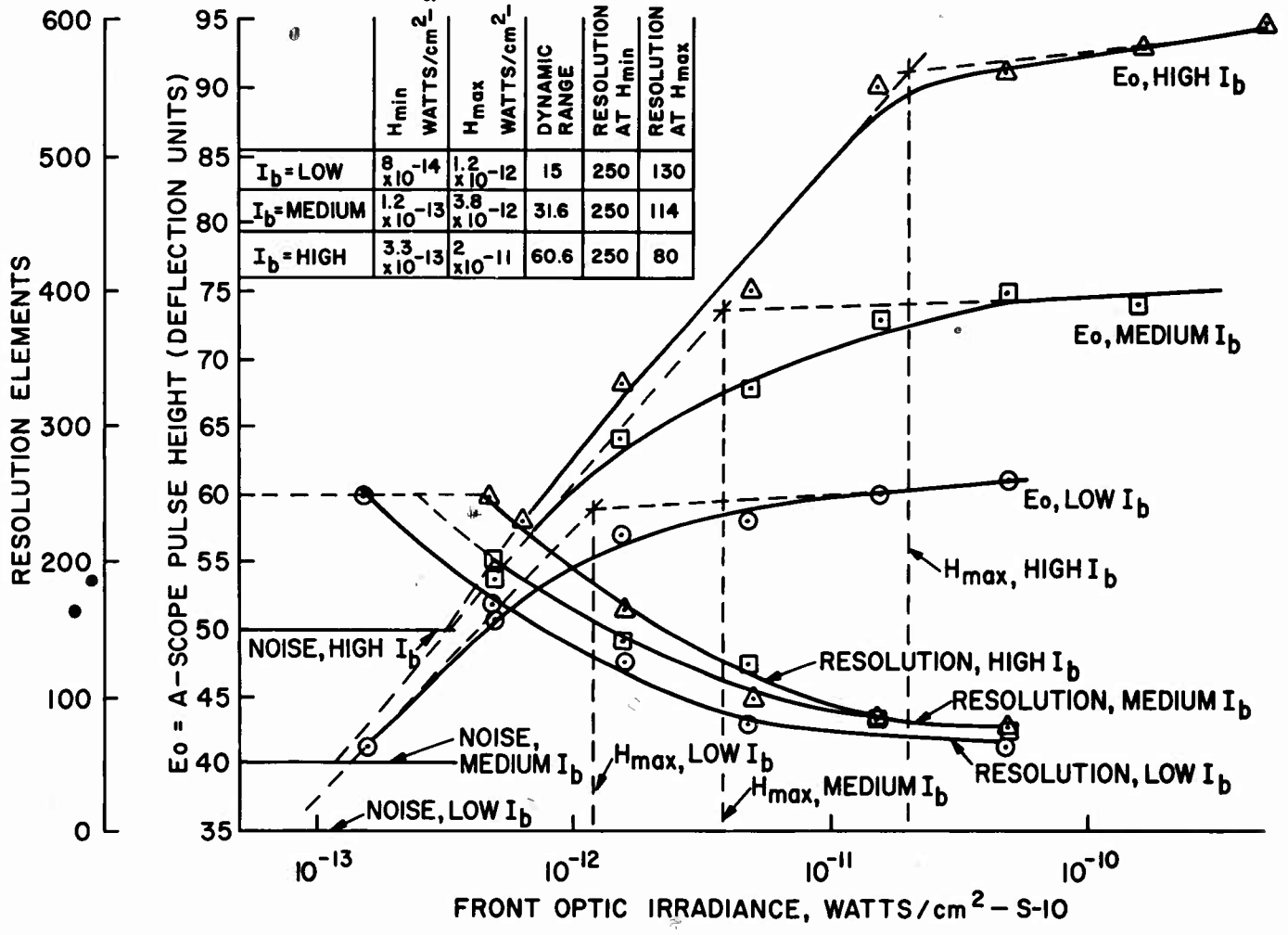

	H_{min} WATTS/cm^2–S10	H_{max} WATTS/cm^2–S10	DYNAMIC RANGE	RESOLUTION AT H_{min}	RESOLUTION AT H_{max}
I_b=LOW	8×10^{-14}	1.2×10^{-12}	15	250	130
I_b=MEDIUM	1.2×10^{-13}	3.8×10^{-12}	31.6	250	114
I_b=HIGH	3.3×10^{-13}	2×10^{-11}	60.6	250	80

Figure 8. System Transfer Functions, ϵ_T = 5.0 Volts

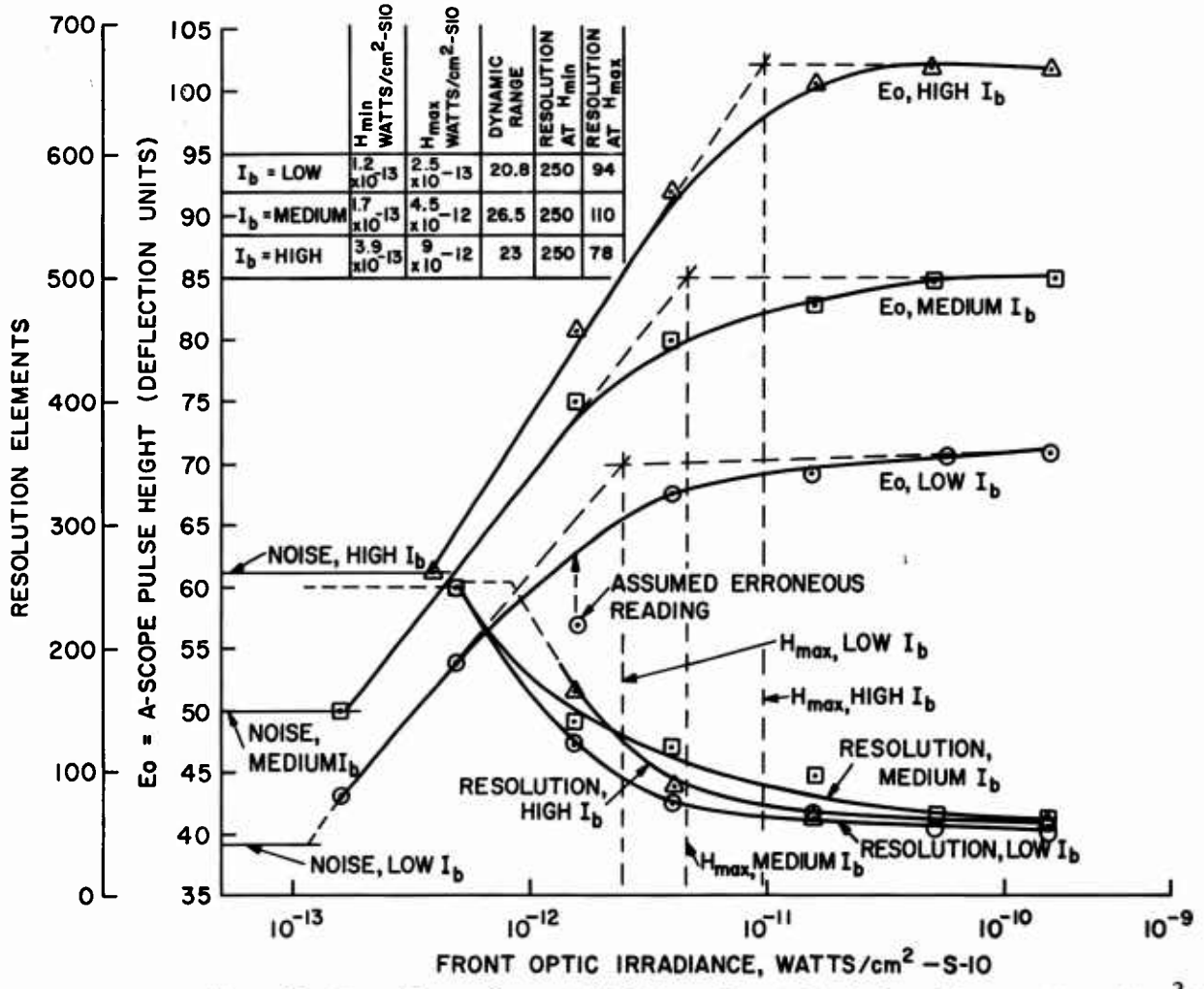

Figure 9. System Transfer Functions, ϵ_T = + 8 Volts. Front Optic Irradiance, Watts/cm^2 S-10

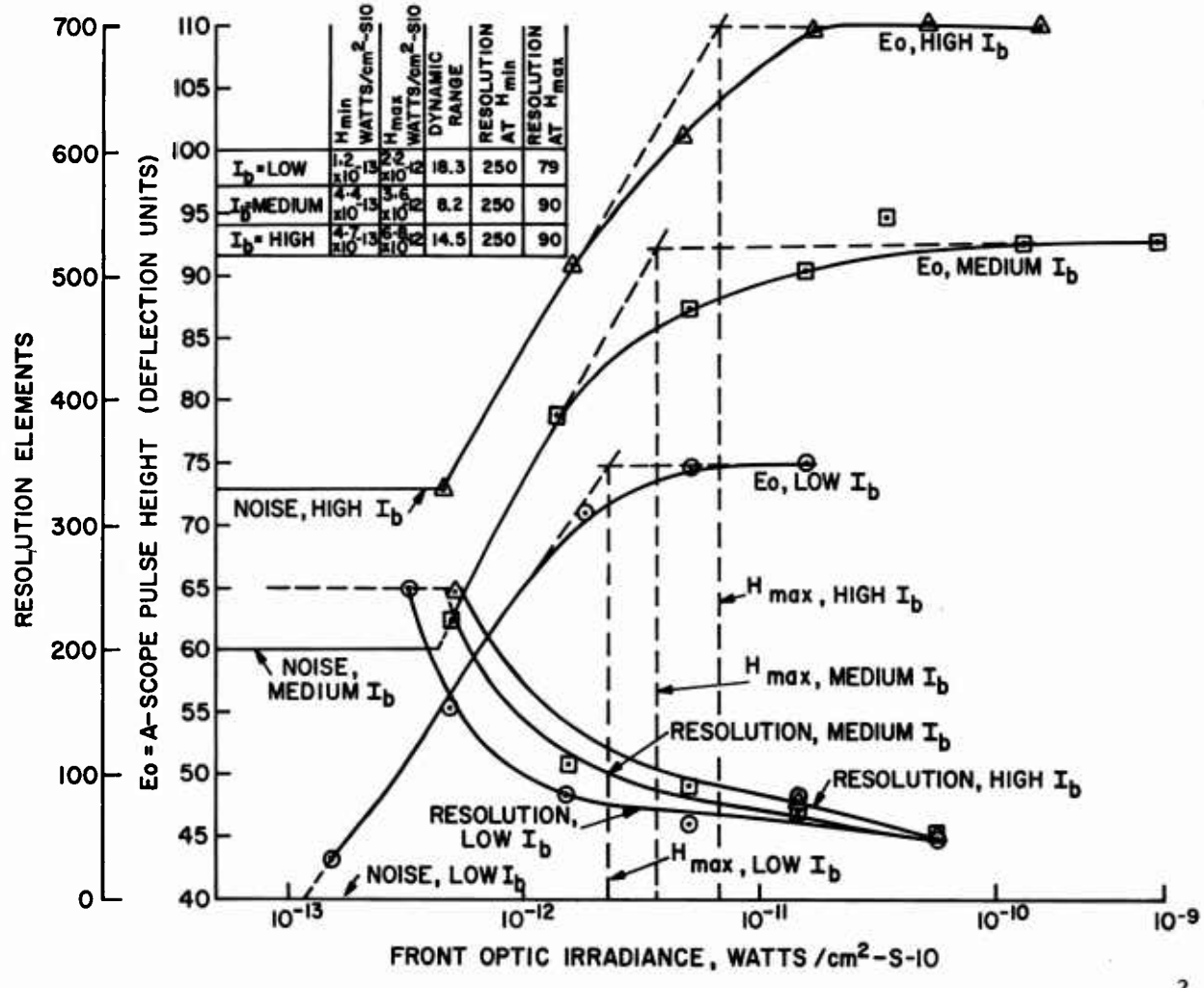

Figure 10. System Transfer Function, ϵ_T = + 10 Volts. Front Optic Irradiance, Watts/cm^2 S-10

Maximum sensitivities, as obtained at low beam current, are degraded by a factor of 2 to 4 at high beam current conditions.

4. Resolution at the stronger signal levels, which can be most accurately measured and which is more dependent on system adjustment, is best used as a measure of the effect of target voltage and beam current on point target resolution. From the curves, it can be seen that best strong signal resolution is obtained at the higher beam currents and lower target voltages.

It was originally expected that the higher target voltages might allow accumulation of greater target charge prior to the target's reaching mesh potential, and that an according increase in system dynamic range might be thus achievable. This effect was not shown by the experimental data.

Based upon the above observations, operation at +2 volts target potential and medium beam current has been specified for general case operation.

2. Radiometric Accuracy

a. Sensitivity Variation Across the Photocathode Surface

Measurement of relative sensitivity across the photocathode was accomplished by placing a 7-square x 5-square mask on the monitor C-scope, and measuring the A-scope pulse height for target location in the center of each of the 35 squares under the condition of constant input irradiance. The constant irradiance used was approximately midway in the system dynamic range. This measurement was performed first without use of shading correction signals. A later test involved an attempt at using the shading correction generator to reduce the effect of photocathode surface sensitivity variation.

Results of these tests are shown in Figure 11.

As may be seen from the solid curves, without the use of shading corrections, sensitivity relative to that at the photocathode center is 85% or better across a good portion of the photocathode surface. Relative sensitivity at the edges drops to about 75%.

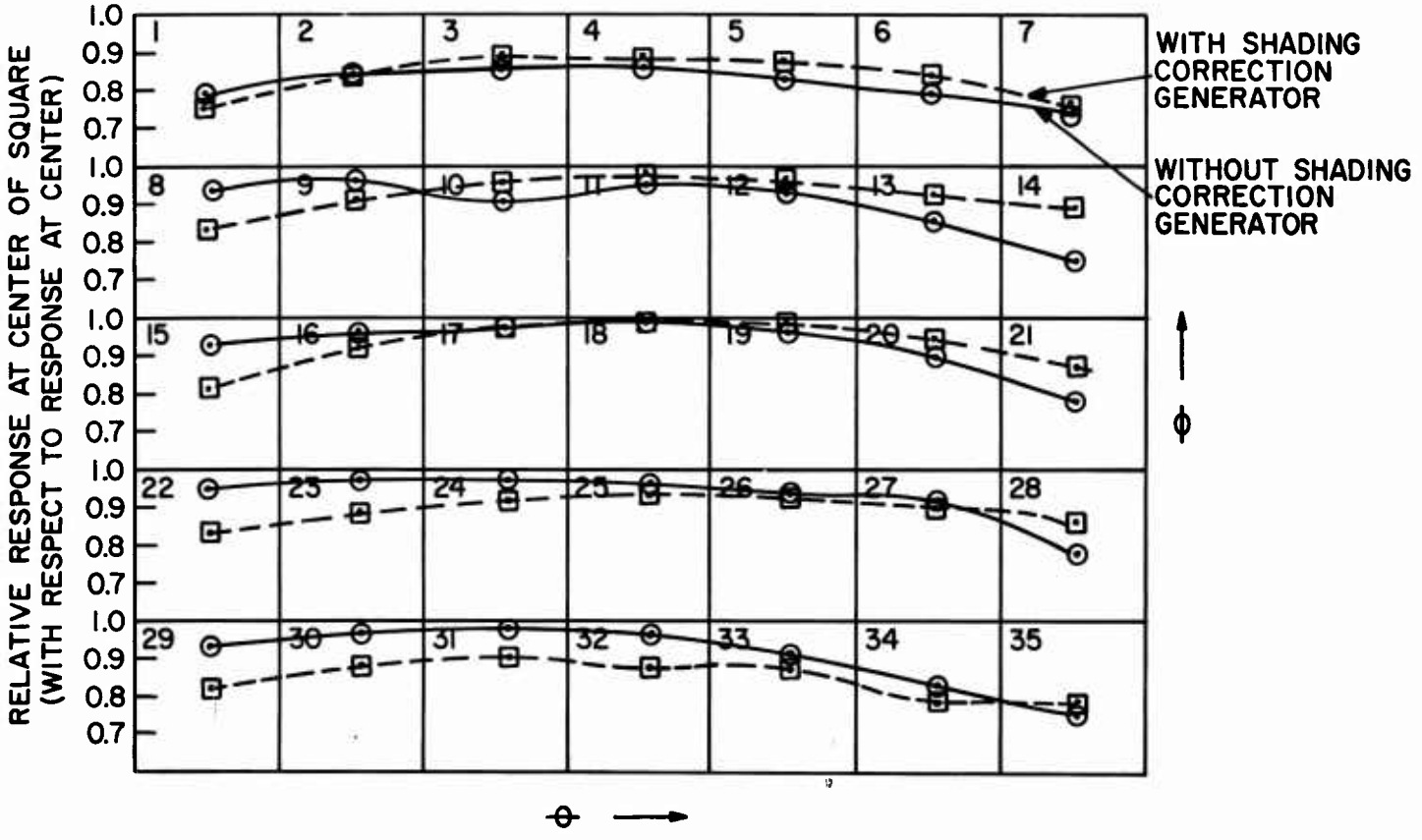

Figure 11. Relative Response Across Photocathode Surface

The dashed curves show a similar measurement taken with the use of shading correction signals. As may be seen, a positive improvement was not obtained. This may be due largely to the fact that insufficient time was available for detailed experimentation with the shading correction generator. This device generates vertical and horizontal saw tooth waveforms of adjustable amplitude, phase, and polarity. These are mixed with the video to provide appropriate shading corrections. This technique should be capable of yielding better performance than indicated by the data shown.

Some question might be raised about the validity of these tests in terms of indicated radiometric instability as discussed in subsequent paragraphs. Inasmuch as the system was "tuned up" prior to each of the two shading tests noted above, and the performance time of the tests was only a few minutes, the data is considered reasonably valid.

b. Calibration Repeatability

Steady-state operation of the image orthicon system against constant source irradiance indicated that calibration drift which is not negligible is occurred over fairly short periods of time. It was observed that control settings, particularly beam alignment and landing, are critical and must be readjusted every five to ten minutes to preserve a constant overall system gain. Without this readjustment, A-scope pulse amplitude was observed to change by a factor of up to 1.5 over a nominal ten minute period. This introduces a maximum calibration error of up to perhaps 35% to 50% in terms of the applicable system transfer function.

The program scope and schedule did not allow detailed investigation of this instability. Subsequent checkout will be performed to further investigate this area.

3. Reciprocity/System Absolute Performance

The image orthicon control panel wiring was modified to provide switchable operation between the original image focus (photocathode potential) and pulsed photocathode modes. For the latter, the trigger amplifier and monostable multivibrator earlier described in this report are switched to the photocathode, along with an adjustable voltage divider to set the d.c. level of the gating waveform.

Standard system calibrations were run under the following conditions:

1. Full-frame integration time using the original image focus circuitry.

2. Pulsed photocathode operation at integration times of 80%, 60%, and 40% of the normal frame time.

The "Standard" operating point of +2 volts target potential and medium beam current was used for these tests. Data was taken against a night sky background which did not provide a significant noise increase over capped lens system noise.

System performance data obtained is shown in Figures 12, 13, 14, and 15. All curves are plotted as a best "eyeball" smoothed fit to the measured data points.

Reciprocity between data obtained using the pulsed mode and the non-pulsed mode was not achieved. A much higher quality image focus is obtained when using the new gating circuitry. This is assumed to cause the non-reciprocity in this case. Nominal reciprocity is noted for the 40% and 60% gated data, with a fall-off in reciprocity for the 80% gated case. This is probably due to a slight decrease in achievable image focus quality for the 80% gated case. This condition can be easily rectified.

Examination of the data shown in the curves indicates that best sensitivities of 1.8×10^{-14} watts/cm^2-S10 are now achieved using the new photocathode bias circuitry. Correction of the slight fall-off in image focus at high pulsed duty cycles should improve this by a factor of about 1.6.

Resolution is noted to reach a maximum of 250 elements. This is assumed to be the limit imposed by beam size.

The data obtained indicates that the straight line extrapolation from the minimum-intensity data point to the noise, formerly used to extend calibration data to the NFFD, is not valid. The actual data exhibits considerable curvature at the low-signal end as well as at the high-signal end. This provides somewhat better sensitivities than those previously estimated.

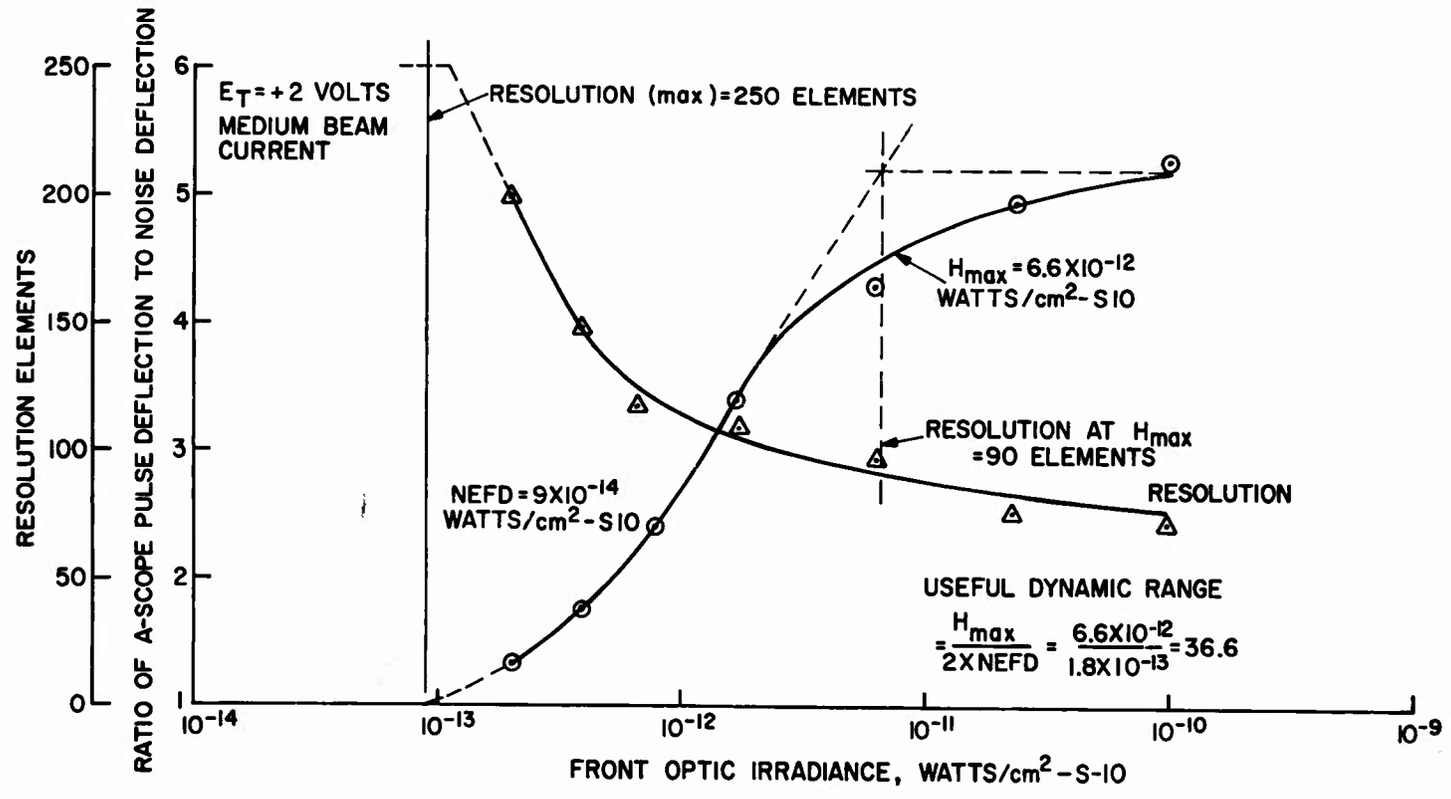

Figure 12. System Performance 100% Integration, Original Image Focus Circuitry

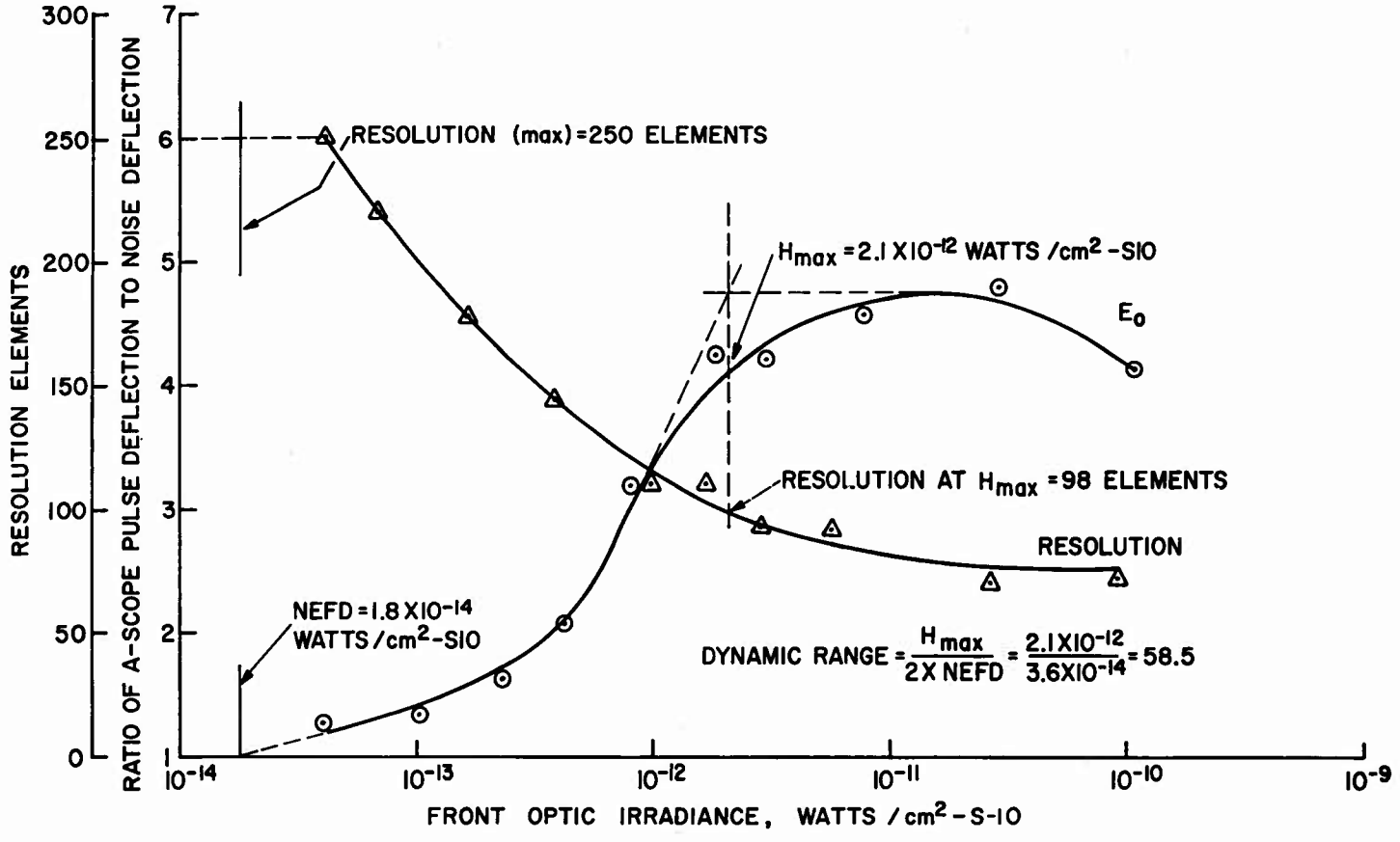

Figure 13. System Performance 80% Integration, Pulsed Photocathode, ϵ_T = + 2 Volts, Medium Beam Current

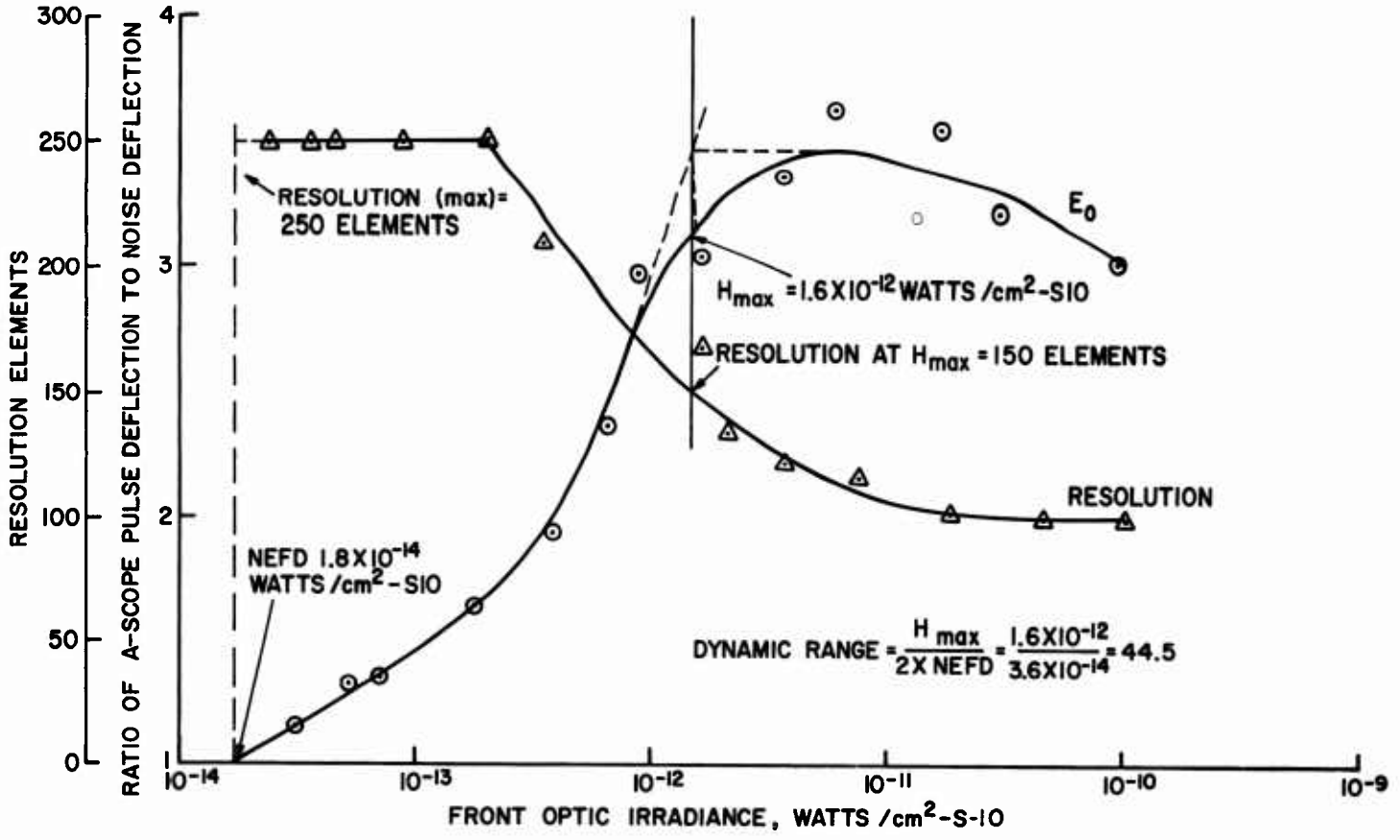

Figure 14. System Performance 60% Integration Time, Pulsed Photocathode, ϵ_T = + 2 Volts, Medium Beam Current

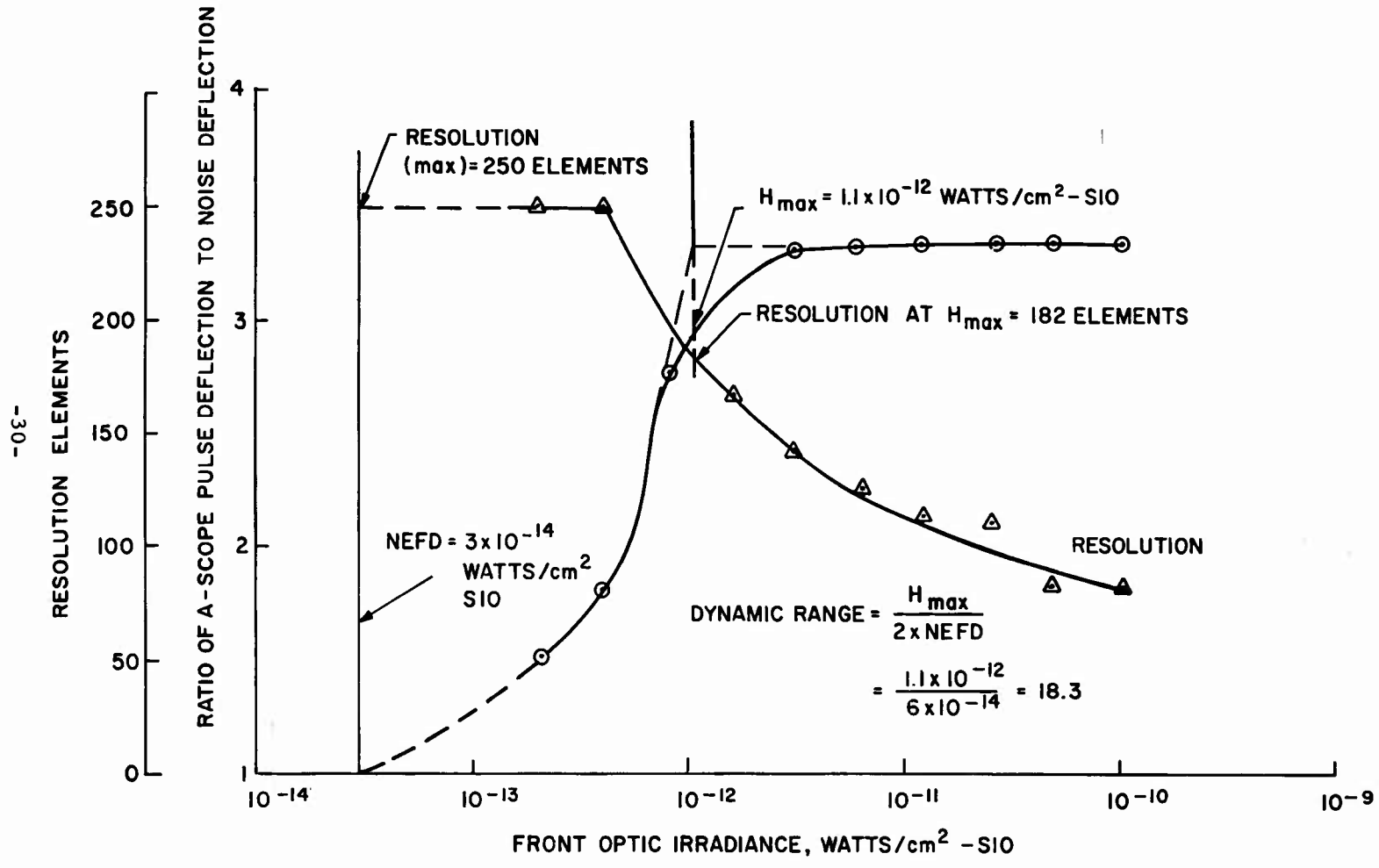

Figure 15. System Performance, 40% Integration Time, Pulsed Photocathode, ϵ_T = +2 Volts, Medium Beam Current

A signal-to-noise ratio of at least two is deemed appropriate to radiometry. Useful dynamic ranges are thus computed using a value of 2 x NEFD for the lower signal limit. Upper limit of dynamic range is taken as the knee of the system response curve. This is subject to interpretation; thus dynamic range figures are considered representative of achievable performance rather than as exact figures.

Resolution, as plotted here, was determined by the same techniques and criteria used for the previously described measurements of the effect of beam current and target voltage on system operation.

UNCLASSIFIED